Absorption and fluorescence in frequency-modulated fields under conditions of strong modulation and saturation

N. Nayak and G. S. Agarwal
School of Physics, University of Hyderabad, Hyderabad 500134, Andhra, India
(Received 12 July 1984)

The dynamical behavior of a two-level system in an intense frequency-modulated field is obtained without recourse to the weak-modulation assumption. Solutions to the optical Bloch equations are expressed in terms of continued fractions involving 2×2 matrices. Such matrix-continued fractions are numerically evaluated to obtain a wide variety of absorption and fluorescence spectra in frequency-modulated fields. Results in various special cases involving combinations of weak fields, weak modulation, strong modulation, and strong fields are given. Analytical results for weak fields but with an arbitrary degree of modulation are also presented. The spectra exhibit additional resonances for strong modulation. The main resonance shifts and broadens considerably due to strong modulation and saturation effects.

I. INTRODUCTION

Frequency modulation (FM) spectroscopy has become a very standard tool in ultrahigh-resolution spectroscopy.[1–8] Its chief advantage at large modulation frequencies lies in its ability[4,5] to produce signals free from low-frequency noise and thus the resonance profiles can be studied with good signal-to-noise ratio. The work so far in this area has been done under the assumption that the modulation index is very low so that only the signals to the leading order in modulation have been calculated.[4–7] From the point of view of comparing experimental line shapes with theoretical shapes it is important to know the combined effect of strong modulation and of saturation on the frequency-modulated signals. This is studied in detail in this paper. The organization of this paper is as follows. In Sec. II, we rewrite Bloch equations by transforming them to a new frame rotating with the instantaneous frequency of the field. The solution of the transformed Bloch equations is obtained in terms of the *matrix*-continued fractions. In Sec. III, the absorption spectra are calculated, whereas Sec. IV calculates the fluorescence spectra in FM fields. The numerical results are presented for saturating as well as nonsaturating fields. No specific assumption on the strength of the modulation is made. The effect of increasing modulation is to enhance the strength of the signals in *weak* FM fields. Analytical results in this case are presented. The effect of the strong fields and strong modulation is to lead to many new additional resonances in the spectra. The main peak shows remarkable broadening and shift as the modulation index M increases.

II. SOLUTIONS OF OPTICAL BLOCH EQUATIONS AS MATRIX-CONTINUED FRACTIONS

We consider a two-level atom with states $|1\rangle$ and $|2\rangle$ having the energy separation $\hbar\omega_0$. The atom interacts with an intense electromagnetic field whose frequency is modulated in time. The electric field of the radiation can be represented as

$$\mathbf{E}(t)=\mathscr{E}e^{-i[\omega_l t+\phi(t)]}+\text{c.c.}\ , \tag{2.1}$$

where ω_l is the laser frequency and

$$\phi(t)=M\sin(\Omega t) \tag{2.2}$$

with M and Ω being the modulation index and modulation frequency, respectively. We present the two-level atom by the Pauli operators S^+, S^- and S^z. The atom-field interaction in the dipole approximation can be written as

$$V(t)=\hbar g(S^+e^{-i[\omega_l t+\phi(t)]}+S^-e^{i[\omega_l t+\phi(t)]})\ , \tag{2.3}$$

where

$$g=-\mathbf{d}\cdot\mathscr{E}/\hbar \tag{2.4}$$

and $\mathbf{d}$ being the dipole matrix element, which is assumed to be real. In this representation, the optical Bloch equations describing the dynamics of the atom can be written as

$$\begin{aligned}
\langle\dot{S}^+\rangle&=\left[i\omega_0-\frac{1}{T_2}\right]\langle S^+\rangle-2ige^{i[\omega_l t+\phi(t)]}\langle S^z\rangle\ ,\\
\langle\dot{S}^-\rangle&=\left[-i\omega_0-\frac{1}{T_2}\right]\langle S^-\rangle+2ige^{-i[\omega_l t+\phi(t)]}\langle S^z\rangle,\\
\langle\dot{S}^z\rangle&=(\eta-\langle S^z\rangle)/T_1-ige^{-i[\omega_l t+\phi(t)]}\langle S^+\rangle\\
&\quad+ige^{i[\omega_l t+\phi(t)]}\langle S^-\rangle\ ,
\end{aligned} \tag{2.5}$$

where η is the equilibrium value of the atomic population $\langle S^z\rangle$. The relaxation times T_1 and T_2 represent the decay of the population and the dipole moment, respectively. The angular bracket $\langle\cdots\rangle$ represents the ensemble average. Going over to the rotating frame by the transformation

$$\begin{aligned}
\tilde{S}^+&=\langle S^+\rangle e^{-i\omega_l t-i\phi(t)}\ ,\\
\tilde{S}^-&=\langle S^-\rangle e^{+i\omega_l t+i\phi(t)}\ ,\\
\tilde{S}^z&=\langle S^z\rangle\ ,
\end{aligned} \tag{2.6}$$

we get the dynamical equations for slowly varying quantities

$$\dot{\underline{X}}=\underline{A}(t)\underline{X}+\underline{I}\ , \tag{2.7}$$

where

$$\underline{A}=\begin{bmatrix} i\Delta-\frac{1}{T_2}-i\mu(t) & 0 & -2ig \\ 0 & -i\Delta-\frac{1}{T_2}+i\mu(t) & 2ig \\ -ig & ig & -\frac{1}{T_1} \end{bmatrix}, \tag{2.8}$$

$$\underline{X}=\begin{bmatrix} \tilde{S}^{+} \\ \tilde{S}^{-} \\ \tilde{S}^{z} \end{bmatrix},\quad \underline{I}=\begin{bmatrix} 0 \\ 0 \\ \eta/T_1 \end{bmatrix}, \tag{2.9}$$

and

$$\mu(t)=\dot{\phi}(t)=M\Omega\cos(\Omega t),\quad \Delta=\omega_0-\omega_l\ . \tag{2.10}$$

It is thus seen that frequency modulation of the laser field adds an extra detuning factor which varies in time. Because of this, the exact solution of Eq. (2.7) has not been so far obtained. Solutions are known[4–10] for weak modulation, but the field can be of arbitrary intensity. Here we present the solution which is valid for arbitrary strength of the field and for arbitrary values of the modulation index.

For this purpose we use the Fourier decomposition

$$\underline{X}=\sum_{n=-\infty}^{\infty}\underline{\psi}^{(n)}e^{-in\Omega t}\ , \tag{2.11}$$

where for each value of n, $\underline{\psi}^{(n)}$ is a column matrix. The equations of motion for $\underline{\psi}^{(n)}$ are now given by

$$\dot{\psi}_1^{(n)}=\left[i\Delta+in\Omega-\frac{1}{T_2}\right]\psi_1^{(n)}-\frac{iM\Omega}{2}\psi_1^{(n+1)}-\frac{iM\Omega}{2}\psi_1^{(n-1)}-2ig\psi_3^{(n)}\ , \tag{2.12a}$$

$$\dot{\psi}_2^{(n)}=\left[-i\Delta+in\Omega-\frac{1}{T_2}\right]\psi_2^{(n)}+\frac{iM\Omega}{2}\psi_2^{(n+1)}+\frac{iM\Omega}{2}\psi_2^{(n-1)}+2ig\psi_3^{(n)}\ , \tag{2.12b}$$

$$\dot{\psi}_3^{(n)}=\left[in\Omega-\frac{1}{T_1}\right]\psi_3^{(n)}-ig\psi_1^{(n)}+ig\psi_2^{(n)}+I_3\delta_{n,0}\ . \tag{2.12c}$$

We find that Eqs. (2.12) couple $\underline{\psi}^{(n)}$ with $\underline{\psi}^{(n\pm1)}$. In the steady state ($\dot{\underline{\psi}}^{(n)}=\underline{0}$), on eliminating $\psi_3^{(n)}$ and using

$$\underline{\phi}_n=\begin{bmatrix}\psi_1^{(n)}\\ \psi_2^{(n)}\end{bmatrix}, \tag{2.13}$$

we get the equation

$$\underline{A}_n\underline{\phi}_n+b\underline{B}_0\underline{\phi}_{n+1}+b\underline{B}_0\underline{\phi}_{n-1}=\delta_{n,0}\underline{r}_0\ , \tag{2.14}$$

where

$$\underline{A}_n=\begin{bmatrix} \frac{1}{T_2}-a_n-i\Delta-in\Omega & a_n \\ a_n & \frac{1}{T_2}-a_n+i\Delta-in\Omega \end{bmatrix}, \tag{2.15}$$

$$\underline{B}_0=\begin{bmatrix}1 & 0\\ 0 & -1\end{bmatrix} \tag{2.16}$$

with

$$a_n=2g^2\left[in\Omega-\frac{1}{T_1}\right]^{-1},\quad b=\frac{iM\Omega}{2},\qquad \underline{r}_0=-2ig\eta\begin{bmatrix}1\\ -1\end{bmatrix}. \tag{2.17}$$

We now present the solution of (2.14) in terms of the matrix-continued fraction. For this purpose we define

$$\underline{P}_n=(\underline{B}_0)^{-1}\underline{A}_n \text{ and } \underline{\phi}_n=\underline{Z}_n(\underline{B}_0)^{-1}\underline{r}_0\ . \tag{2.18}$$

This gives us the equation for $\underline{Z}_n$

$$\underline{P}_n\underline{Z}_n+b\underline{Z}_{n+1}+b\underline{Z}_{n-1}=\delta_{n,0}\underline{I}\ . \tag{2.19}$$

We further define

$$\underline{X}_n=\underline{Z}_n(\underline{Z}_{n-1})^{-1} \tag{2.20}$$

and obtain from (2.19) the recursion relation for $n\neq0$,

$$\underline{P}_n+b\underline{X}_{n+1}+b(\underline{X}_n)^{-1}=\underline{0} \tag{2.21}$$

and hence

$$\underline{X}_n=-b(\underline{P}_n+b\underline{X}_{n+1})^{-1},\quad n\neq0\ . \tag{2.22}$$

This can be written for $\underline{Y}_{-n}=(\underline{X}_{-n})^{-1}$ in the form

$$\underline{Y}_{-n}=-b(\underline{P}_{-n-1}+b\underline{Y}_{-n-1})^{-1}\ . \tag{2.23}$$

Equation (2.19) yields, for $n=0$, the expression

$$\underline{Z}_0=[\underline{P}_0+b\underline{X}_1+b(\underline{X}_0)^{-1}]^{-1}\ . \tag{2.24}$$

The matrix (X_0^{-1}) can be obtained from Eq. (2.21) with $n=-1$,

$$(\underline{X}_0)^{-1}=-b(\underline{P}_{-1}+b\underline{Y}_{-1})^{-1}\ . \tag{2.25}$$

Equations (2.22)–(2.25) give us $\underline{Z}_0$ and hence we can calculate $\underline{Z}_1,\underline{Z}_2,\ldots$ from Eq. (2.20). This in turn can be used to obtain $\underline{\psi}^{(n)}$. It may be noted here that the matrix-continued fraction involves $\underline{P}_n$'s which are 2×2 matrices. We have not used any approximation (except the rotating-wave approximation) in deriving Eqs. (2.22)–(2.25) and hence the results are valid for arbitrary strength of the laser field and modulation. The continued fractions [Eqs. (2.22) and (2.23)] which shall be used for further study in this paper are of the form

$$\underline{X}_1=\cfrac{-b}{\underline{P}_1+\cfrac{\beta}{\underline{P}_2+\cfrac{\beta}{\underline{P}_3+\cdots}}} \quad \text{and} \quad \underline{Y}_{-1}=\cfrac{-b}{\underline{P}_{-2}+\cfrac{\beta}{\underline{P}_{-3}+\cfrac{\beta}{\underline{P}_{-4}+\cdots}}} , \tag{2.26}$$

where $\beta=M^2\Omega^2/4$. This shows that $\underline{X}_1$ and $\underline{Y}_{-1}$ are odd functions of M as $\underline{P}_n$'s are M independent. Hence $\underline{Z}_0$, given by Eq. (2.24), is an even function of M. Given $\underline{Z}_0$, $\underline{Z}_1$ can be obtained from Eqs. (2.20) and (2.24):

$$\underline{Z}_1=\underline{X}_1\underline{Z}_0 , \tag{2.27}$$

which is seen to be an odd function of M. With the help of these equations we will derive the expressions for the fluorescence and absorption spectra of a two-level system in frequency-modulated fields.

III. ABSORPTION SPECTRA IN FREQUENCY-MODULATED BEAMS

In this section we show how the formulation of Sec. II can be used to obtain absorption spectra in FM fields of arbitrary intensity and modulation index. The atomic polarization is, by definition,

$$\mathbf{p}=\mathbf{d}\langle S^+\rangle+\text{c.c.} ,$$

which, on using Eq. (2.6), can be written as

$$\mathbf{p}=\mathbf{d}\tilde{S}^+ e^{i\omega_l t+i\phi(t)}+\text{c.c.} \tag{3.1}$$

On using the Fourier decomposition (2.11), the polarization becomes

$$\mathbf{p}=\sum_{n=-\infty}^{\infty}\mathbf{d}\psi_1^{(n)}e^{i\omega_l t+i\phi(t)-in\Omega t}+\text{c.c.} \tag{3.2}$$

The rate of absorption of energy from the FM field can be calculated by using (3.2) and the rate at which fields do work.[11] An algebraic calculation shows that

$$\frac{dW}{dt}=\mathbf{E}\cdot\frac{d\mathbf{p}}{dt}=2g\hbar\omega_l\text{Im}\psi_1^{(0)}+2g\hbar\omega_l\sum_{n=1}^{\infty}[(\text{Im}\psi_1^{(n)}-\text{Im}\psi_2^{(n)})\cos(n\Omega t)-(\text{Re}\psi_1^{(n)}-\text{Re}\psi_2^{(n)})\sin(n\Omega t)] , \tag{3.3}$$

where g is given by Eq. (2.4). In obtaining (3.3) small correction terms have been ignored by assuming $\omega_l \gg M\Omega,\Omega$. Equation (3.3) shows that the absorption rates contain components varying sinusoidally at all harmonics of the modulation frequency Ω. The d.c. component proportional to $\text{Im}\psi_1^{(0)}$ also depends on the modulation frequency. In what follows, we will only be interested in the components at Ω:

$$\frac{dW^{(1)}}{dt}=2g\hbar\omega_l[A_c\cos(\Omega t)+A_s\sin(\Omega t)] , \tag{3.4}$$

where

$$A_c=\text{Im}\psi_1^{(1)}-\text{Im}\psi_2^{(1)} , \tag{3.5}$$

$$A_s=\text{Re}\psi_2^{(1)}-\text{Re}\psi_1^{(1)} . \tag{3.6}$$

$\psi_1^{(1)}$ and $\psi_2^{(1)}$ can be obtained from expressions (2.20) and (2.22)–(2.25). On using Eqs. (2.11), (2.26), and (2.27), the symmetry properties of $\psi_1^{(n)}$ and $\psi_2^{(n)}$ as a function of Ω are found to be

$$\psi_1^{(n)}(-\Omega)=-[\psi_2^{(n)}(\Omega)]^* , \tag{3.7a}$$

$$\psi_2^{(n)}(-\Omega)=-[\psi_1^{(n)}(\Omega)]^* \tag{3.7b}$$

for odd values of n and

$$\psi_1^{(n)}(-\Omega)=[\psi_2^{(n)}(\Omega)]^* , \tag{3.7c}$$

$$\psi_2^{(n)}(-\Omega)=[\psi_1^{(n)}(\Omega)]^* \tag{3.7d}$$

for even values of n. These relations lead to the following for the in-phase and quadrature components:

$$A_c(-\Omega)=-A_c(\Omega) , \tag{3.8a}$$

$$A_s(-\Omega)=A_s(\Omega) . \tag{3.8b}$$

The behavior of $\psi_1^{(n)}$ and $\psi_2^{(n)}$ with Δ can easily be proved using the two equations in (2.14) and (3.7) and is found to be

$$\psi_1^{(n)}(-\Delta)=\psi_2^{(n)}(\Delta) , \tag{3.9a}$$

$$\psi_2^{(n)}(-\Delta)=\psi_1^{(n)}(\Delta) \tag{3.9b}$$

for odd values of n and

$$\psi_1^{(n)}(-\Delta)=-\psi_2^{(n)}(\Delta) , \tag{3.10a}$$

$$\psi_2^{(n)}(-\Delta)=-\psi_1^{(n)}(\Delta) \tag{3.10b}$$

for even values of n. In view of (3.9), we find the following symmetry property of A_c and A_s:

$$A_c(-\Delta)=-A_c(\Delta) , \qquad A_s(-\Delta)=-A_s(\Delta) . \tag{3.11}$$

We next present the results for A_c and A_s obtained from the numerical evaluation of the matrix-continued fractions of Sec. II. For numerical check, we have compared the results for weak modulation ($M \ll 1$) with the results obtained earlier.[7] We consider the two cases corresponding to the weak and strong fields separately.

A. Weak field and arbitrary modulation

When the field is weak, some of the typical absorption spectra are shown in Fig. 1. One finds absorption or dispersion structure centered at $\Omega=\Delta$. As M increases, the signals no longer remain linear in M. In the weak-

field limit, the width of the signals is practically independent of the modulation index M.

In the weak-field limit the signals can be calculated analytically for arbitrary values of M. From (3.3) it is clear that we need to calculate $\psi_1^{(n)}$, etc., to first order in g and hence Eq. (2.8) for $\tilde{S}^+$ can be linearized, i.e.,

$$\dot{\tilde{S}}^+ = \left[i\Delta - \frac{1}{T_2} - i\mu(t) \right] \tilde{S}^+ - 2ig\eta \ . \tag{3.12}$$

The long-time solution of (3.12) can be shown to be

$$\tilde{S}^+(t) = -2ig\eta \sum_{n,m} J_n(M) J_m(M) \times \left[\frac{1}{T_2} - i\Delta + in\Omega \right]^{-1} e^{i(n-m)\Omega t} , \tag{3.13}$$

where $J_n(M)$ is the Bessel function of order n and hence

$$\psi_1^{(1)} = -2ig\eta \sum_{n=-\infty}^{+\infty} J_n(M) J_{n+1}(M) \times \left[\frac{1}{T_2} - i\Delta + in\Omega \right]^{-1} . \tag{3.14}$$

Similarly one can show that

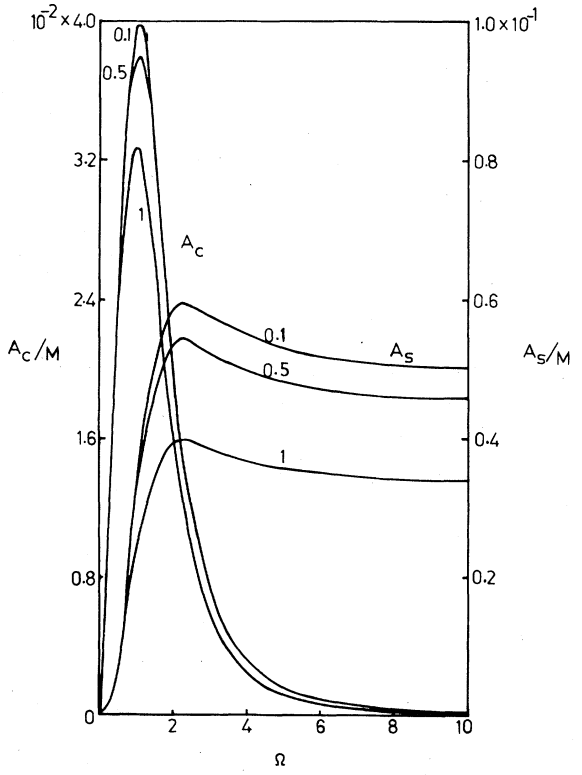

FIG. 1. Modulation frequency dependence of the in-phase and the quadrature components A_c and A_s of the modulated absorption at Ω in weak fields $g=0.1$ and with increasing values of the modulation index M. All the parameters are in units of T_2 and in all numerical calculations T_1 has been set as 0.5. Different curves are labeled by the values of M and $\Delta=1.0$.

$$\psi_2^{(1)} = 2ig\eta \sum_{n=-\infty}^{+\infty} J_n(M) J_{n-1}(M) \times \left[\frac{1}{T_2} + i\Delta - in\Omega \right]^{-1} . \tag{3.15}$$

The analytical results for A_c and A_s are obtained by substituting (3.14) and (3.15) in (3.5) and (3.6). We find, for example, the in-phase component A_c

$$A_c = \frac{-2g\eta}{T_2} \sum_{n=-\infty}^{+\infty} J_n(M)[J_{n+1}(M) + J_{n-1}(M)] \times \left[\left[\frac{1}{T_2} \right]^2 + (\Delta - n\Omega)^2 \right]^{-1} . \tag{3.16}$$

We thus find that A_c, in the Ω scan (Δ fixed), will show absorption structures at $\Omega=\Delta/n$, each with width $(1/T_2 n)$. The weight factor of the structure at $\Omega=\Delta/n$ is proportional to

$$J_n(M)[J_{n+1}(M) + J_{n-1}(M)].$$

Note that all the resonances will be seen provided that the separation between two successive resonances $\Delta/n - \Delta/(n+1)$ is much bigger than

$$\frac{1}{T_2} \left[\frac{1}{n} + \frac{1}{n+1} \right] .$$

For the parameters of Fig. 1, one sees only the resonance $\Omega=\Delta$ with a weight factor proportional to $2J_1^2(M)/M$. The peak heights of Fig. 1 are in agreement with this weight factor. The quadrature component obviously has a similar behavior.

B. Strong field and arbitrary modulation

If both the field strength and the modulation index are large, then the situation is very complex. We show the numerical results for the in-phase and quadrature components in Figs. 2–5. We present the modulated absorp-

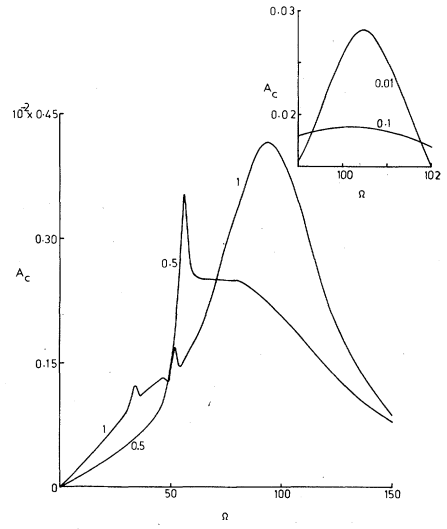

FIG. 2. The in-phase component A_c as a function of the modulation frequency for strong fields $g=50.0$ and for $\Delta=10$. The inset shows A_c for weak modulation.

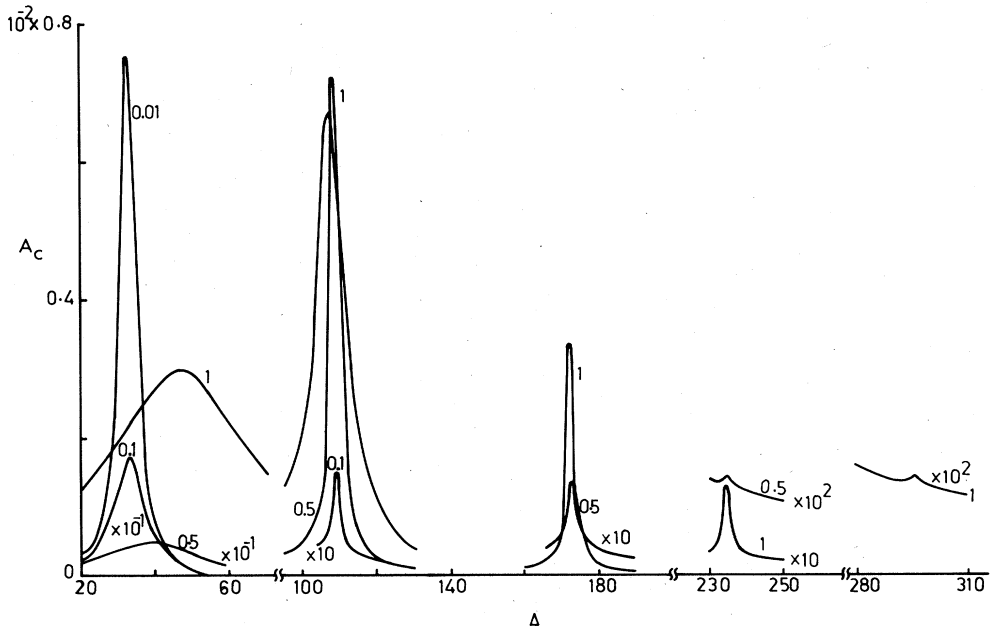

FIG. 3. The scan of A_c as a function of detuning $\Delta=\omega_0-\omega_l$ for fixed $\Omega(=60)$ and the intensity ($g=25$) of the field. The modulation index is varied. Different curves are on different scales. The symbol "$\times 10^n$" indicates that the curve has been amplified 10^n times.

tion spectra as a function of the modulation frequency as well as the detuning. The in-phase components (quadrature components) are predominantly absorption (dispersion) type. The spectra of Figs. 2–5 show that as the modulation index increases, additional resonant structures start appearing. For example, for weak M, one has the structures at

$$\Omega=\pm(4g^2+\Delta^2)^{1/2}\ .$$

As M increases, the structures corresponding to subharmonics of this value, i.e., for

$$\frac{1}{n}(4g^2+\Delta^2)^{1/2}$$

start appearing. This can be understood from the structure of the FM field (2.1) which can be written as

$$E(t)=\mathscr{E}\sum_{-\infty}^{+\infty}J_n(M)e^{-i(\omega_l+n\Omega)t}+\text{c.c.} \tag{3.17}$$

Thus the radiation field is a superposition of fields with frequencies $\omega_l+n\Omega$ and with intensities $|\mathscr{E}J_n(M)|^2$. Thus as M increases, the components $\omega_l+n\Omega$ for few low n values start becoming strong and hence the resonances corresponding to the subharmonics

$$\Omega\sim\frac{1}{n}(4g^2+\Delta^2)^{1/2}$$

start showing up. This value of Ω corresponds to the vanishing of the determinant of the matrix P_n defined by (2.18). It may also be seen from Fig. 3 that the main peak $\Omega=(4g^2+\Delta^2)^{1/2}$ shows considerable "power broadening" and shifts as the modulation index increases.[12] For low

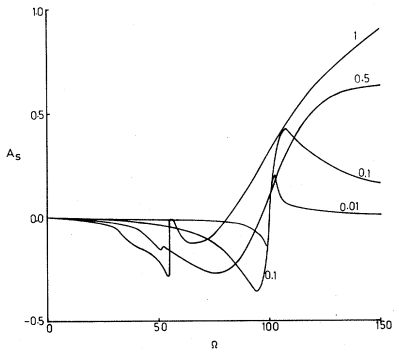

FIG. 4. The quadrature component A_s as a function of Ω for different degrees of modulation and for strong fields. Other parameters are as in Fig. 2.

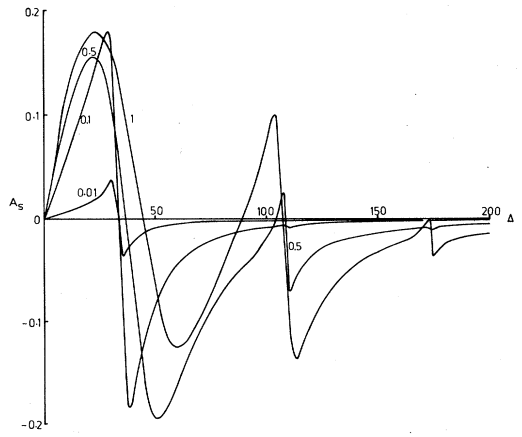

FIG. 5. Same as in Fig. 4, except that now the detuning is varied; other parameters are same as in Fig. 3.

values of the modulation the width of the main peak in $A_c(\Delta)$ can be approximately obtained even for strong fields from the zero of the determinant $P_1(\Omega > 2g)$ and is found to be

$$\frac{1}{T_2}\left[1-\frac{4g^2}{\Omega^2}\right]^{-1/2}\left[1-\frac{2g^2}{\Omega^2}\left[1-\frac{T_2}{T_1}\right]\right] .$$

IV. FLUORESCENCE SPECTRA IN FREQUENCY-MODULATED FIELDS

In this section we use the formulation of Sec. II to obtain the structure of the fluorescence spectra[8,9,13] in FM beams with arbitrary degree of modulation. The fluorescence $I(t)$ produced by our two-level system is proportional to the population in the excited state, which in turn can be expressed in terms of $\langle S^z(t)\rangle$,

$$I(t)=\rho_{11}(t)=\tfrac{1}{2}+\langle S^z(t)\rangle . \tag{4.1}$$

On using (2.11), Eq. (4.1) reduces to

$$I(t)=\tfrac{1}{2}+\sum_{-\infty}^{+\infty}\psi_3^{(n)}e^{in\Omega t} \tag{4.2}$$

which on using $\psi_3^{(n)*}=\psi_3^{-(n)}$ reduces to

$$I(t)=\tfrac{1}{2}+2\,\mathrm{Re}\psi_3^{(0)}+2\sum_{n=1}^{\infty}[\mathrm{Re}\psi_3^{(n)}\cos(n\Omega t) +\mathrm{Im}\psi_3^{(n)}\sin(n\Omega t)] . \tag{4.3}$$

As before we will deal only with the component oscillating at Ω. Thus the in-phase component (quadrature component) $I_c(I_s)$ will be equal $\mathrm{Re}\psi_3^{(1)}(\mathrm{Im}\psi_3^{(1)})$. The function $\psi_3^{(1)}$ can be obtained from (2.12c) in terms of $\psi_1^{(1)}$, $\psi_2^{(1)}$, which already have been evaluated

$$\psi_3^{(1)}=(\psi_1^{(1)}-\psi_2^{(1)})ig\left[i\Omega-\frac{1}{T_1}\right]^{-1} . \tag{4.4}$$

The symmetry properties of I_c and I_s under the change in sign of Δ and Ω can be found from (4.4), (3.7), and (3.9):

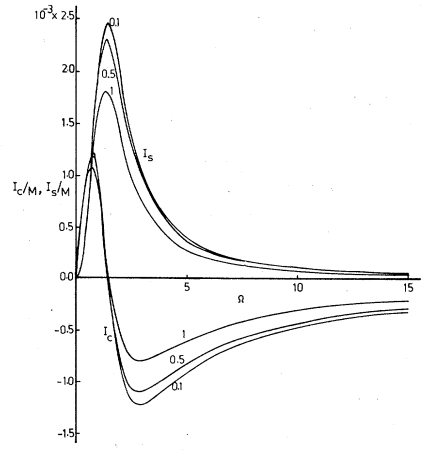

FIG. 6. The fluorescence spectra in modulated fields as a function of modulation frequency for weak fields $g=0.1$ and for $\Delta=1.0$. Different curves are for varying degrees of modulation.

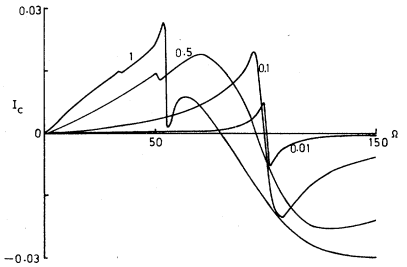

FIG. 7. The in-phase component I_c of fluorescence as a function of modulation frequency for strong fields $g=50$, $\Delta=10$; curves are labeled by the value of M.

$$\psi_3^{(n)}(-\Omega)=-[\psi_3^{(n)}(\Omega)]^* ,$$
$$\psi_3^{(n)}(-\Delta)=-\psi_3^{(n)}(\Delta) \tag{4.5}$$

for odd n and

$$\psi_3^{(n)}(-\Omega)=[\psi_3^{(n)}(\Omega)]^* ,$$
$$\psi_3^{(n)}(-\Delta)=\psi_3^{(n)}(\Delta) \tag{4.6}$$

for even n. On using (4.5) and (4.6) in (4.3) we find the results

$$I_c(-\Omega)=-I_c(\Omega),\quad I_s(-\Omega)=+I_s(\Omega) , \tag{4.7}$$

$$I_c(-\Delta)=-I_c(\Delta),\quad I_s(-\Delta)=-I_s(\Delta) . \tag{4.8}$$

The results of numerical calculations on fluorescence are presented separately in the two cases. The numerical program has been checked against the known analytical results[9] in the case of weak modulation.

A. Weak field and arbitrary modulation

For weak fields and increasing degree of modulation, the fluorescence spectra are shown in Fig. 6. The spectra show more or less similar behavior as M increases except that the nonlinearities in M start setting in. The in-phase component has dispersionlike structure. The computed spectra can be understood from the analytical results. The function $S^z(t)$ can be calculated to second order in g from the solutions already given in Sec. III. On using (4.4), (3.14), (3.15), and a number of simplifications one can show that

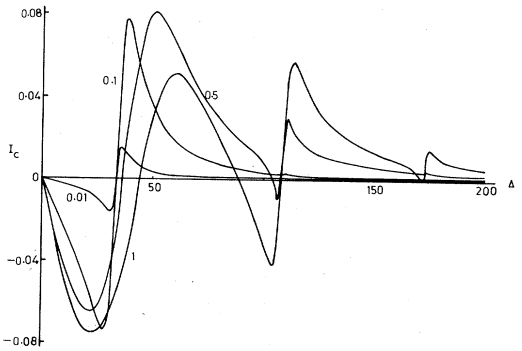

FIG. 8. I_c as a function of detuning Δ for fixed $\Omega=60$ and $g=25$.

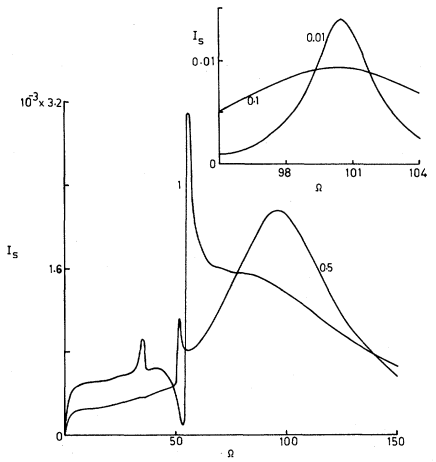

FIG. 9. The quadrature component I_s of fluorescence as a function of Ω for parameters same as in Fig. 7. The inset shows the result for weak modulation.

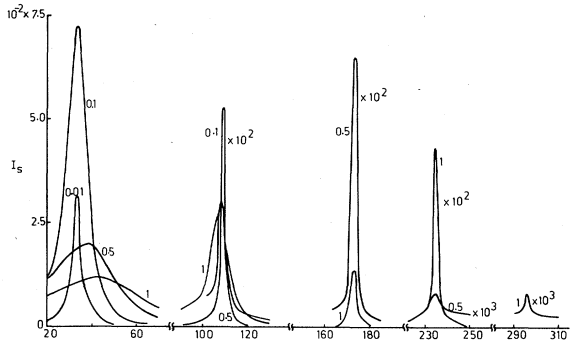

FIG. 10. I_s as a function of Δ for fixed $\Omega=60$, $g=25$. Curves have been drawn on different scales. The label "$\times 10^n$" on a curve indicates that the curve has been amplified 10^n times.

$$I_c=+4g^2\eta\left[\left[\frac{1}{T_1}\right]^2+\Omega^2\right]^{-1}\sum_n J_n(M)\left[\left[\frac{1}{T_2}\right]^2+(\Delta-n\Omega)^2\right]^{-1}\left[2\Omega(\Delta-n\Omega)J_n'(M)+\frac{2n\Omega}{MT_1T_2}J_n(M)\right], \tag{4.9}$$

$$I_s=-4g^2\eta\left[\left[\frac{1}{T_1}\right]^2+\Omega^2\right]^{-1}\sum_n J_n(M)\left[\left[\frac{1}{T_2}\right]^2+(\Delta-n\Omega)^2\right]^{-1}\left[\frac{2\Omega n}{MT_2}J_n(M)-\frac{2(\Delta-n\Omega)}{T_1}J_n'(M)\right], \tag{4.10}$$

$$J_n'(M)=\frac{d}{dM}J_n(M)\ .$$

The numerical results of Fig. 6 are consistent with the above analytical results. Unlike the absorption spectra, the fluorescence, in phase component, say, has, in general, both absorption and dispersion structure depending on the parameters of the system.

B. Strong field and strong modulation

The results obtained from the numerical evaluation of the matrix-continued fraction of Sec. II are shown in Figs. 7–10. Both Ω and Δ scan are given. The in-phase components (quadrature components) have the dispersion (absorption) structure. The characteristics of the fluorescence spectra are very similar to those of the absorption spectra of Sec. III. We, for example, find the appearance of new resonances corresponding to $n^2\Omega^2=4g^2+\Delta^2$ as the degree of modulation increases. The power broadening and shift of the main peak with increase in M is also to be noticed. The similarities of fluorescence and absorption spectra can be understood from Eq. (4.4). For large modulation frequencies $\Omega \gg 1/T_1$, we have

$$\psi_3^{(1)}\approx\left[\frac{g}{\Omega}\right](\psi_1^{(1)}-\psi_2^{(1)}) \tag{4.11}$$

and hence from (3.4) and (4.3) we find the relation between absorption and fluorescence spectra in modulated beams,

$$I_c(\Delta)=-\frac{g}{\Omega}A_s(\Delta)\ ,$$
$$I_s(\Delta)=\frac{g}{\Omega}A_c(\Delta)\ . \tag{4.12}$$

The numerical results shown in Figs. 3, 5, 8, and 10 are in confirmation with (4.12).

ACKNOWLEDGMENT

This work is partially supported by a grant from the Department of Science and Technology, Government of India.

[1]C. L. Tang and J. M. Telle, J. Appl. Phys. **45**, 4503 (1974); E. I. Moses and C. L. Tang, Opt. Lett. **1**, 115 (1977).

[2]S. A. Akhmanov, Y. D. Golyosv, and S. V. Lambralov, Kvant. Elektron. (Moscow) **5**, 1329 (1978) [Sov. J. Quantum Electron. **8**, 758 (1978)].

[3]Y. A. Barashev, V. M. Senibalamat, and E. A. Titov, Kvant. Elektron. (Moscow) **6**, 261 (1979) [Sov. J. Quantum Electron. **9**, 141 (1979)].

[4]G. C. Bjorklund, Opt. Lett. 5, 15 (1980); G. C. Bjorklund and M. D. Levenson, Phys. Rev. A **24**, 166 (1981); G. C. Bjorklund, M. D. Levenson, W. Lenth, and C. Ortiz, Appl. Phys. **B32**, 145 (1983).

[5]J. L. Hall, L. Hollberg, T. Baer, and H. G. Robinson, Appl. Phys. Lett. **39**, 680 (1981); J. H. Shirley, Opt. Lett. **7**, 537

(1982).
[6]A. Schenzle, R. G. Devoe, and R. G. Brewer, Phys. Rev. A **25**, 2606 (1982).
[7]G. S. Agarwal, Phys. Rev. A **23**, 1375 (1981).
[8]W. Lenth, C. Ortiz, and G. C. Bjorklund, Opt. Commun. **41**, 369 (1982).
[9]G. S. Agarwal, J. Opt. Soc. Am. (to be published).
[10]Exact results in some special cases of the field modulation are given in A. E. Kaplan, Zh. Eksp. Teor. Fiz. **68**, 823 (1975) [Sov. Phys.—JETP **41**, 409 (1976)].
[11]R. Kubo, J. Phys. Soc. Jpn. **12**, 570 (1957); B. R. Mollow, Phys. Rev. A **5**, 2217 (1972).
[12]This behavior is reminiscent of the behavior of a two-level system in an extremely strong radio-frequency field, where one sees multiphoton processes, shifts (Bloch-Siegert type) of resonances, etc., due to counter-rotating terms [cf. J. Shirley, Phys. Rev. **138**, B979 (1965); T. Yabuzaki, S. Nakayama, Y. Murakami, and T. Ogawa, Phys. Rev. A **10**, 1955 (1974)].
[13]Fluorescence in amplitude-modulated beams has been extensively studied. See, for example, L. Armstrong and S. Feneuille, J. Phys. B **8**, 546 (1975); S. Feneuille, M. G. Schweighofer, and G. Oliver, *ibid.* **9**, 2003 (1976); W. A. McClean and S. Swain, *ibid.* **9**, 2011 (1976); R. Saxena and G. S. Agarwal, *ibid.* **12**, 1939 (1979); **13**, 453 (1980); D. T. Pegg, *ibid.* **16**, 2135 (1983).